

Unfolding Features of Bovine Testicular Hyaluronidase Studied by Fluorescence Spectroscopy and Fourier Transformed Infrared Spectroscopy

Nina Pan,¹ Xiaoqiang Cai,¹ Kai Tang,¹ and Guolin Zou^{1,2}

Received March 21, 2005; accepted September 8, 2005
Published online: November 15, 2005

Chemical unfolding of bovine testicular hyaluronidase (HAase) has been studied by fluorescence spectroscopy and Fourier transformed infrared spectroscopy (FTIR). Thermodynamic parameters were determined for unfolding HAase from changes in the intrinsic fluorescence emission intensity and the formations of several possible unfolding intermediates have been identified. This was further confirmed by representation of fluorescence data in terms of 'phase diagram'. The secondary structures of HAase have been assigned and semiquantitatively estimated from the FTIR. The occurrence of conformational change during chemical unfolding as judged by fluorescence and FTIR spectroscopy indicated that the unfolding of HAase may not follow the typical two-state model.

KEY WORDS: Hyaluronidase; chemical unfolding; fluorescence; phase diagram; FTIR.

INTRODUCTION

The term hyaluronidase has been used to denote a group of enzymes from different sources that catalyze the depolymerization of hyaluronate (HA), a certain acidic glycosaminoglycans [1]. HA composed of repeating disaccharide units of D-glucuronic acid and N-acetyl-D-glucosamine is now recognized as a major participant in such important biological processes as cell motility, proliferation, differentiation, and migration [2]. There are three main groups of enzymes with this specificity, but with different reaction mechanisms, i.e., (i) testicular-type hyaluronidase (hyaluronoglucosaminidase; hyaluronate 4-glycanohydrolase, EC 3.2.1.35), (ii) leech hyaluronidase (hyaluronate glycanohydrolase, EC 3.2.1.36), and (iii) bacterial hyaluronidase (hyaluronate lyase EC 4.2.2.1) [3]. The HAase present in various mammalian tissues, belonging to the first group, are of particular biological interest since

they have been demonstrated to be involved in the pathophysiology of many human disorders such as cancer and rheumatoid arthritis [4]. The level of HAase was significantly increased in breast tumor metastases as compared to primary tumor [5]. Due to their physiological importance, the features for the unfolding of HAase have increasingly attracted attention.

The major goal of this study was to clarify the unfolding features of HAase induced by guanidinium chloride (GdnHCl) and urea. Chemical denaturants such as GdnHCl and urea are widely used for study of the thermodynamics of protein unfolding [6]. Results of unfolding experiments were carry out in the presence or absence of reductants [7]. The unfolding behavior of the HAase induced by GdnHCl and urea in the presence or absence of 2-mercaptoethanol has been analyzed by monitoring intrinsic fluorescence, including emission intensity, shift of λ_{\max} and parameter *A* value which is characteristic of the energy range and the vibronic progression of the fluorescence spectra [8]. The formation of possible unfolding intermediates was further confirmed by representation of intrinsic fluorescence data in terms of a 'phase diagram', i.e., I_{λ_1} versus I_{λ_2} dependence, where I_{λ_1} and I_{λ_2} are the fluorescence emission intensity values measured at

¹ State Key Laboratory of Virology, Department of Biotechnology, College of Life Sciences, Wuhan University, Wuhan, 430072, China

² To whom correspondence should be addressed. E-mail: zouguolin@whu.edu.cn

wavelengths λ_1 and λ_2 under different experimental conditions [9].

The developments in FTIR spectroscopy of proteins have led to their successful application to study the secondary structures of proteins, and satisfactory results have been obtained for the contents of different secondary structures compared with the structures in the crystalline state by X-ray diffraction studies [10]. One of the advantages of this method is its sensitivity for slight change of protein conformation. It is the purpose of the present study to examine the changes in the secondary structures of HAase during chemical unfolding [11].

Chemical unfolding is a useful technique to determine the modification of the protein stability by effect of the medium conditions, or recently by the mutation of amino acids from the wild-type protein. The unfolded state of a protein is an ensemble of microscopic conformations. To further elucidate the structural features of HAase, the unfolding process was investigated using very sensitive measurements of protein intrinsic fluorescence and FTIR spectroscopy.

MATERIALS AND METHODS

Materials

Bovine testicular HAase (EC 3.2.1.35; 300 NFU/mg) was purchased from Sigma. Co. D₂O was bought from Johnson Matthey Co. All other chemicals were of analytical reagent grade. All aqueous solutions were prepared using water filtered through a Milli-Q water system (Millipore, Bedford, MA, USA).

Equilibrium Unfolding Experiments

HAase was dissolved in 0.1 M sodium phosphate buffer (pH 5.8) [12] and the final protein concentration was 0.1 mg/mL for the fluorescence experiments. Small aliquots of this stock solution were added to the reaction mixture containing the desired concentrations of GdnHCl or urea in the presence or absence of the reductant (0.5 mM 2-mercaptoethanol). Protein solutions were incubated at 4°C for 12 hr to reach the equilibrium.

Emission Fluorescence Spectra of Unfolded HAase

The fluorescence measurements were performed on an F-4500 spectrofluorimeter (Hitachi, Japan) at 25°C. The sample was excited at 295 nm where tryptophan residue is excited. Both the excitation and emission slits

were set at 5 nm. The energy range and vibronic progression of the fluorescence spectra were characterized by the parameter $A = (I_{320}/I_{365})_{295}$, where I_{320} and I_{365} are fluorescence intensities at 320 and 365 nm, respectively [9].

'Phase Diagram' Method

The 'phase diagram' method, which was elaborated by Burstein for the analysis of fluorescence data, is extremely sensitive for the detection of any intermediate state [7,9]. The essence of this method is to build up the diagram of I_{λ_1} versus I_{λ_2} , where I_{λ_1} and I_{λ_2} are the fluorescence intensity values measured on wavelengths λ_1 and λ_2 under different experimental conditions for a protein undergoing structural transformations. Fluorescence intensity was recorded at 320 and 365 nm (the same as for parameter A).

It has been noted that the dependence of $I(\lambda_1) = f(I(\lambda_2))$ will be linear if changes in the protein environment lead to all-or-none transition between two different conformations. In the context of protein, all-or-none should be identified as structurally all-native or non-native. The thermodynamics of such a structural transition is two-state [13]. On the other hand, non-linearity of this function reflects the sequential character of structural transformations. Moreover, each linear portion of the $I(\lambda_1) = f(I(\lambda_2))$ dependence will describe individual all-or-none transitions.

Fourier Transformed Infrared Spectroscopy Study of HAase Secondary Structure

HAase was dissolved in D₂O with different concentrations of GdnHCl for measurements of FTIR spectra obtained with a NEXUS 670 (Thermo Nicolet) infrared spectrophotometer. The final concentration of protein was 7.5 mg/mL. The sample chamber was thoroughly dried by a current of dry air for 1 hr before the commencement of spectral scan. The spectra were usually scanned 64 times in the experiment [14].

Difference spectra for protein were generated by subtraction of the spectra of buffer from the observed spectra of the protein solution to satisfy the criterion that a straight baseline was obtained from 2000 to 1800 cm⁻¹ [15]. The Fourier self-deconvolution was performed using a Bio-Rad program with EZ OMNIC Version 5.2.

RESULTS AND DISCUSSION

Intrinsic Fluorescence

Fluorescence emission spectra of HAase measured in different conditions are shown in Fig. 1. Native HAase

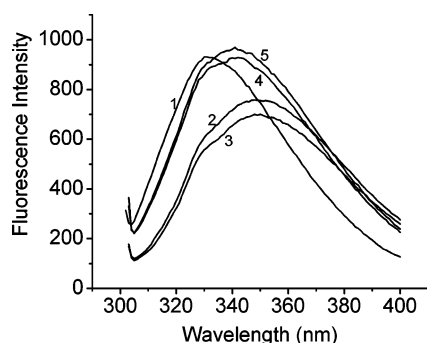


Fig. 1. Fluorescence emission spectra of HAase excited at 295 nm. (1) no denaturant; (2) 6 M GdnHCl; (3) 6 M GdnHCl, 0.5 mM 2-mercaptoethanol; (4) 8 M urea; (5) 8 M urea, 0.5 mM 2-mercaptoethanol.

contains more than thirty tryptophan residues located dispersedly around the protein [16]. At 25°C HAase has fluorescence maximum at 332 nm, indicating that tryptophan residues are rather protected from the aqueous solvent [17]. After 8.0 M urea was added, the λ_{\max} shifts to 340 nm, due to an increase in tryptophan residues exposure. This effect is even greater in 6.0 M GdnHCl, where the tryptophan residues are mostly exposed to water (maximum at 347 nm). As commonly found, GdnHCl is a stronger denaturant than urea [18]. Samples unfolded by urea have a little higher fluorescence intensities compared to native HAase, while the ones unfolded by GdnHCl are much lower. Reductant does not hamper these shifts of λ_{\max} since there is nearly the same increase in tryptophan residues exposure in the presence or absence of 0.5 mM 2-mercaptoethanol. The changes of fluorescence intensity effect by 2-mercaptoethanol have been taken out.

The maximum emission λ_{\max} was monitored at different concentrations of denaturant and unfolding curves were built in Fig. 2. Urea mainly destroys the hydrophobic chains that keep the stability of protein structure. The fluorescence intensity may increase slightly than native HAase along with the weakening of hydrophobic property. Whereas GdnHCl contains positively charged guanidine group, inter- or intra-molecular hydrogen bonds could be cleaved and rearranged [19]. Therefore, the extent of GdnHCl induced unfolding is much greater than urea. The tryptophan residues are at their greatest exposure to the environment [20] with λ_{\max} of 347 nm after addition of 6.0 M GdnHCl. The conformation of HAase is stable in GdnHCl below 0.2 M, corresponding to the native state. Between 1.0 and 3.5 M GdnHCl a modest change in tryptophan residue environment is observed. There is a small increase in λ_{\max} from 332 nm to 333 nm, which indicated that the protein is reasonably stable over this range of denaturant concentrations. Another important stable in-

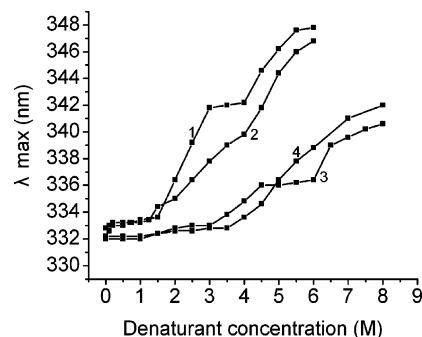


Fig. 2. λ_{\max} shift of unfolding curve. (1) GdnHCl induced; (2) GdnHCl induced, contain 0.5 mM 2-mercaptoethanol; (3) urea induced; (4) urea induced, contain 0.5 mM 2-mercaptoethanol.

termediate state with λ_{\max} of 342 nm is visible in about 4.0 M GdnHCl. A similar intermediate state with λ_{\max} of 333 nm is still visible by treatment of HAase with 3.0 M urea. However, in this case, the tryptophan residues could not reach the greatest exposure till in 8.0 M urea.

Figure 2 also shows HAase unfolding in the presence of the reductant (0.5 mM 2-mercaptoethanol). The extent of unfolding is basically close to the corresponding samples without the reductant. Interestingly, all the stable intermediate states are inconspicuous in 0.5 mM 2-mercaptoethanol.

Figure 3 illustrates GdnHCl induced changes in parameter A ($A = I_{320}/I_{365}$, which is characteristic of the shape and the position of the fluorescence spectra [9]), of HAase over a wide range of denaturant concentrations in the presence or absence of the reductant. Parameter A gradually decreases and reaches a plateau in the vicinity of 0.1–1.0 M GdnHCl. However, a further increase of denaturant concentration leads to a pronounced decrease in the parameter A value, which is over at 4.0–5.0 M GdnHCl. Thus, data for the GdnHCl dependence of parameter A reflect an accumulation of two intermediates, maximally populated in the vicinity of 1.0 M and 4.0 M GdnHCl, respectively. Nevertheless, there is no visible plateau in the decrease of parameter A when adding 0.5 mM 2-mercaptoethanol. Figure 3B shows a similar parameter A curve obtained by the treatment of HAase with urea. The plateau in 3.0–4.0 M urea also becomes invisible when adding 0.5 mM 2-mercaptoethanol.

Non-linear least-squares have been used to fit α (the unfolded fraction) versus the denaturant concentration curves. The concentration of the denaturant at the midpoint of unfolding (C_m) was determined applying the following equation:

$$\alpha = \frac{F_N^0 - F_i}{F_N^0 - F_U^0} \quad (1)$$

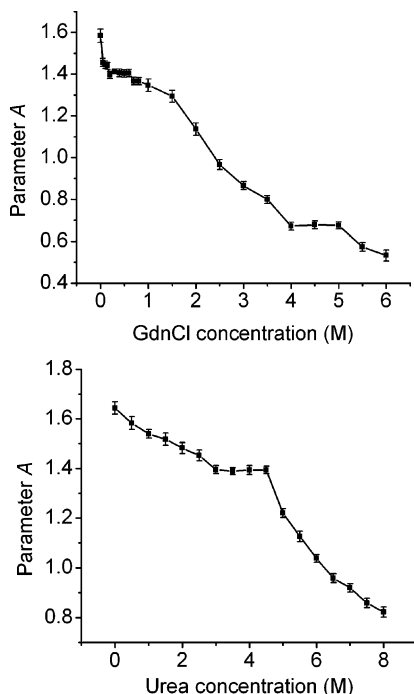


Fig. 3. GdnHCl induced changes in intrinsic fluorescence parameter A . Fluorescence was excited at 295 nm. Protein concentration was 0.1 mg/mL. Protein was incubated in 0.1 M sodium phosphate buffer pH 5.8 in the presence of the desired GdnHCl concentration at 4°C for 12 hr to reach the equilibrium. Measurements were carried out at 25°C. The figure represents results of at least three independent experiments.

where, F_N^0 and F_U^0 are the fluorescence intensity maximum of the native (in the absence of denaturant) and unfolded states (at high denaturant concentration), respectively and F_i is the fluorescence of the protein at i concentration of denaturant [21]. According to Eq. (1), the data of α versus GdnHCl concentration were shown in Fig. 4, which showed that HAase had achieved its completed unfolded state accompanied by hydrophobic residues exposure in 6 M GdnHCl.

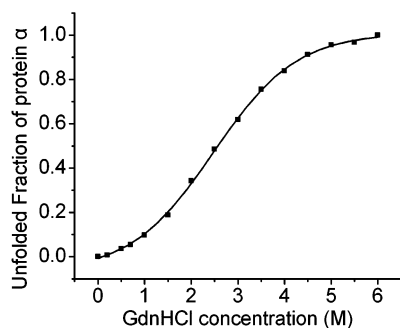


Fig. 4. GdnHCl unfolded fraction of HAase. Protein concentration was 0.1 mg/mL. The buffers used are the same as those shown in Fig. 3.

'Phase Diagram' Analysis of HAase Fluorescence Spectra

The essence of this method is to build up the diagram of I_{λ_1} versus I_{λ_2} . As the fluorescence intensity is the extensive parameter, it will describe any two-component system by a simple relationship:

$$I(\lambda_1) = a + bI(\lambda_2) \quad (2)$$

where

$$a = I_1(\lambda_1) - \frac{I_2(\lambda_1) - I_1(\lambda_1)}{I_2(\lambda_2) - I_1(\lambda_2)} I_1(\lambda_2)$$

and

$$b = \frac{I_2(\lambda_1) - I_1(\lambda_1)}{I_2(\lambda_2) - I_1(\lambda_2)}$$

where $I_1(\lambda)$ and $I_2(\lambda)$ are the fluorescence intensities of the first and second components at given wavelength. In application to protein unfolding, Eq. (2) predicts that the dependence $I(\lambda_1) = f(I(\lambda_2))$ will be linear if changes in protein environment lead to the all-or-none transition between two different conformations. Alternatively, the non-linearity of this function reflects the sequential character of structural transformations. Moreover, each linear portion of the $I(\lambda_1) = f(I(\lambda_2))$ dependence will describe an individual all-or-none transition [9,13,22]. In principle λ_1 and λ_2 are arbitrary wavelengths of the fluorescence spectra, but in practice such diagrams will be more informative if λ_1 and λ_2 will be on different slopes of the spectra such as 320 and 365 nm.

Figure 5 gives additional support to the idea that GdnHCl induced unfolding of HAase is an exceptionally complex process. This figure was designed using the method of 'phase diagram.' It clearly shows that the phase diagram plotted for the GdnHCl induced unfolding of HAase consists of three linear parts, in which the concentration of GdnHCl is 0–1.0 M, 1.0–4.0 M, 4.0–6.0 M, respectively. This reflects the existence of at least three independent transitions separating four different conformational states, including native state, unfolded state, and two possible intermediate states, and further corroborates the results of λ_{\max} shift and parameter A value. Similarly, when adding 0.5 mM 2-mercaptoethanol, the intermediate state in 1.0 M GdnHCl was invisible. Interestingly, λ_{\max} shift and parameter A value did not detect the intermediate state populated in the vicinity of 4.0 M GdnHCl in the presence of 0.5 mM 2-mercaptoethanol.

Native HAase is a single polypeptide contains two disulfide bonds [16] that contribute for the stability of secondary structure. 2-Mercaptoethanol can cleave the disulfide bonds, and it may go against the formations of several possible unfolding intermediates.

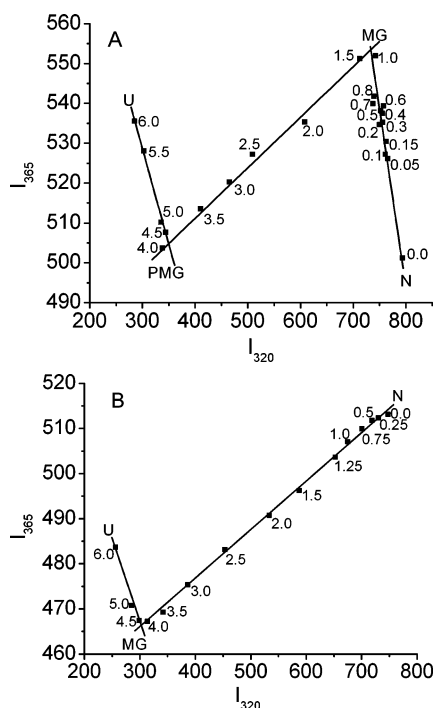


Fig. 5. Phase diagram representing the unfolding of HAase induced by an increase in GdnHCl concentration. GdnHCl concentration values are indicated in the vicinity of the corresponding symbol. (A) contain GdnHCl only; (B) contain 0.5 mM 2-mercaptoethanol and GdnHCl. Each straight line represents an all-or-none transition between two conformers. N and U denote native and unfolded protein respectively; MG and PMG denote two possible intermediate states.

FTIR Spectra of HAase

The infrared chemical denaturation studies of HAase were performed in different GdnHCl concentration. The gradual changes in amide I' of the original spectra after digital subtraction of HAase with increasing denaturant concentrations are shown in Fig. 6. The peak of the original amide I' shift to lower wave numbers and becomes more unsymmetric during denaturation, indicating structural changes.

The major band in amide I' of native HAase (no denaturant, 25°C) is at 1643.1 cm^{-1} , resulting from the strong hydrogen bonding interaction [23]. The band height decreases with the increase of GdnHCl concentration. The transition occurs between 0 M and 3.0 M GdnHCl concentration, and the peak of amide I' shifts to 1641.2 cm^{-1} .

Figure 7 shows the effect of different concentration of GdnHCl on the amide I' in Fourier self-deconvolution spectra in 1700–1600 cm^{-1} region of HAase in D_2O buffer. Based upon many previous studies [24–26], the amide I' band components of protein can be assigned as

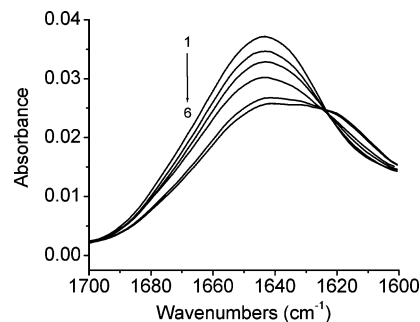


Fig. 6. Original FTIR spectrum of HAase in D_2O of (1) 0 M; (2) 0.5 M; (3) 1.0 M; (4) 1.5 M; (5) 2.0 M; (6) 3.0 M GdnHCl. Concentration of HAase was 7.5 mg/mL.

follows: The bands at 1633.4, 1645, 1652.7 cm^{-1} are assigned to extended strand, irregular (random) structures and α -helix structures, respectively. The bands at 1664.3 and 1689.4 cm^{-1} are assigned to turn structures.

The spectra of chemical denatured state show the following characteristics. There are several almost entirely distributed component bands. The lower height and broader halfwidth of these bands indicate the absence of typical regular structures [27]. In other words, all of the fine structures, such as α -helix and turns, decrease at high concentration of GdnHCl.

An interesting phenomenon attracts our attention that the whole area of original amide I' decreases with the increase of GdnHCl concentration accompanying the unfolding of HAase. This result can be partly explained by the difference in absorption coefficients for the structures at different GdnHCl concentration. It also suggests that the absorption coefficients of unordered structures are lower than those of ordered structures.

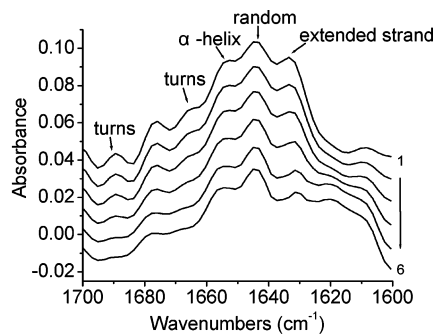


Fig. 7. Fourier self-deconvolution spectrum of HAase. (1) 0 M; (2) 0.5 M; (3) 1.0 M; (4) 1.5 M; (5) 2.0 M; (6) 3.0 M GdnHCl. Concentration of HAase was 7.5 mg/mL.

Thus, our data are consistent with the whole process of chemical induced unfolding of HAase, which takes into account both structural perturbations and disintegration. This unfolding process includes native state, two intermediate states and unfolded state. The first intermediate state may be the molten globule monomer with partial α -helix and turns breakdown. The second intermediate state may be the pre-molten globule more close to unfolded state, which majority of the secondary structure has been disintegrated.

CONCLUSION

Unfolding of HAase induced by chemical denaturants was studied. The results of the fluorescence spectra show that this process involves at least two possible intermediate states, which accompanied a complete loss of the unique secondary structure, and pronounced red shift of the intrinsic fluorescence spectra. The FTIR spectra study afforded us an opportunity to further characterize the unfolding properties of different secondary structures of HAase. The use of Fourier self-deconvolution spectra indicates all of the fine structures decrease at high denaturant concentration.

ACKNOWLEDGMENTS

The authors gratefully acknowledge the support of this research by grant from National Natural Science Foundation of China (No. 30370366, 30470111). We are also grateful to Mrs. Hu Ling for help with the analysis of FTIR spectra.

REFERENCES

1. G. Kreil (1995). Hyaluronidases—a group of neglected enzymes. *Protein Sci.* **4**, 1666–1669.
2. T. Asteriou, B. Deschrevel, B. Delpech, P. Bertrand, F. Bultelle, C. Merai, and J. C. Vincent (2001). An improved assay for the *N*-Acetyl-D-glucosamine reducing ends of polysaccharides in the presence of proteins. *Anal. Biochem.* **293**, 53–59.
3. I. Muckenschnabel, G. Bernhardt, T. Spruss, B. Dietl, and A. Buschauer (1998). Quantitation of hyaluronidases by the Morgan–Elson reaction: Comparison of the enzyme activities in the plasma of tumor patients and healthy volunteers. *Cancer Lett.* **131**, 13–20.
4. E. J. Menzel and C. Farr (1998). Hyaluronidase and its substrate hyaluronan: Biochemistry, biological activities and therapeutic uses. *Cancer Lett.* **131**, 3–11.
5. L. David, V. Dulong, D. L. Cerf, C. Chauzy, V. Norris, B. Delpech, M. Lamacz, and J. P. Vannier (2004). Reticulated hyaluronan hydrogels: A model for examining cancer cell invasion in 3D. *Matrix Biol.* **23**, 183–193.
6. A. Mazzini, A. Maia, M. Parisi, R. T. Sorbi, R. Ramoni, S. Grolli, and R. Favilla (2002). Reversible unfolding of bovine odorant binding protein induced by guanidinium hydrochloride at neutral pH. *Biochim. Biophys. Acta* **1599**, 90–101.
7. F. Yang, Y. Liang, and F. Yang Jr. (2003). Unfolding of lysozyme induced by urea and guanidine hydrochloride studied by “phase diagram” method of fluorescence. *Acta. Chim. Sin.* **61**, 803–807.
8. H. Qiu and M. Caffrey (2000). The phase diagram of the monoolein/water system: metastability and equilibrium aspects. *Biomaterials* **21**, 223–234.
9. I. M. Kuznetsova, O. V. Stepanenko, K. K. Turoverov, L. Zhu, J. M. Zhou, A. L. Fink, and V. N. Uversky (2002). Unraveling multistate unfolding of rabbit muscle creatine kinase. *Biochim. Biophys. Acta* **1596**, 138–155.
10. M. Severcana, P. I. Harisb, and F. Severcanc (2004). Using artificially generated spectral data to improve protein secondary structure prediction from Fourier transform infrared spectra of proteins. *Anal. Biochem.* **332**, 238–244.
11. W. Dzwolak, M. Kato, A. Shimizu, and Y. Taniguchi (1999). Fourier-transform infrared spectroscopy study of the pressure-induced changes in the structure of the bovine α -lactalbumin: The stabilizing role of the calcium ion. *Biochim. Biophys. Acta* **1433**, 45–55.
12. T. Takahashi and M. Ikegami-Kawai (2003). A fluorimetric Morgan–Elson assay method for hyaluronidase activity. *Anal. Biochem.* **322**, 257–263.
13. H. Qian and S. I. Chan (1996). Interactions between a helical residue and tertiary structures: Helix propensities in small peptides and in native proteins. *J. Mol. Biol.* **261**, 279–288.
14. J. Xiea, C. Rileya, M. Kumara, and K. Chittura (2002). FTIR/ATR study of protein adsorption and brushite transformation to hydroxypatite. *Biomaterials* **23**, 3609–3616.
15. M. Gustianandaa, P. I. Harisb, P. J. Milburnc, and J. E. Greadya (2002). Copper-induced conformational change in a marsupial prion protein repeat peptide probed using FTIR spectroscopy. *FEBS Lett.* **512**, 38–42.
16. Z. M. Housley, G. Miglierini, L. Soldatova, P. J. Rizkallah, U. Muller, and T. Schirmer (2000). Crystal structure of hyaluronidase, a major allergen of bee venom. *Structure* **8**, 1025–1035.
17. E. D. Stasio, P. Bizzarri, F. Misiti, E. Pavoni, and A. Brancaccio (2004). A fast and accurate procedure to collect and analyze unfolding fluorescence signal: The case of dystroglycan domains. *Biophys. Chem.* **107**, 197–211.
18. G. T. DeKoster and A. D. Robertson (1997). Calorimetrically-derived parameters for protein interactions with urea and guanidine-HCl are not consistent with denaturant *m* values. *Biophys. Chem.* **64**, 59–68.
19. Q. Xie, T. Guo, J. Lu, and H. M. Zhou (2004). The guanidine like effects of arginine on aminoacylase and salt-induced molten globule state. *Int. J. Biochem. Cell B* **36**, 296–306.
20. D. J. Tew and S. P. Bottomley (2001). Probing the equilibrium denaturation of the serpin α -antitrypsin with single tryptophan mutants: evidence for structure in the urea unfolded state. *J. Mol. Biol.* **313**, 1161–1169.
21. F. C. Morales and M. L. Bianconi (2001). Influence of the oligomeric state of yeast hexokinase isozymes on inactivation and unfolding by urea. *Biophys. Chem.* **91**, 183–190.
22. F. Du, Y. Liang, B. R. Zhou, Y. Xia, M. C. Kilhoffer, and J. Haiech (2004). Unfolding of creatine kinase induced by acid studied by isothermal titration calorimetry and fluorescence spectroscopy. *Thermochim. Acta* **416**, 17–21.
23. P. I. Haris and F. Severcan (1999). FTIR spectroscopic characterization of protein structure in aqueous and non-aqueous media. *J. Mol. Catal. B-Enzym.* **7**, 207–221.
24. H. M. Farrell Jr., E. D. Wickham, J. J. Unruh, P. X. Qi, and P. D. Hoagland (2001). Second structural studies of bovine caseins: Temperature dependence of β -casein structure as analyzed by circular

- dichroism and FTIR spectroscopy and correlation with micellization. *Food Hydrocolloid*. **15**, 341–354.
25. H. Zhanga, Y. Ishikawab, Y. Yamamoto, and R. Carpentiera (1998). Secondary structure and thermal stability of the extrinsic 23 kDa protein of photosystem II studied by Fourier transform infrared spectroscopy. *FEBS Lett.* **426**, 347–351.
26. M. Cauchy, S. D'Aoust, B. Dawson, H. Rode, and M. A. Hefford (2002). Thermal stability: a means to assure tertiary structure in therapeutic proteins. *Biologicals* **30**, 175–185.
27. L. Xie, G. Z. Jing, and J. M. Zhou (1996). Reversible thermal denaturation of staphylococcal nuclease: A fourier transformed infrared spectrum study. *Arch. Biochem. Biophys.* **328**, 122–128.